

Extended X-Ray Absorption Fine Structure Analysis of Cation Distribution in MnFe_2O_4 Single Crystal Films and Artificial Ferrite Structures

Aria Yang, Vincent G. Harris, Scott Calvin, Xu Zuo, and Carmine Vittoria

Abstract—The cation distribution in MnFe_2O_4 single crystal films and artificial ferrite structures is determined by a multiple-edge analysis of the extended X-ray absorption fine structure (EXAFS) of the manganese and iron absorption edges. Compared with conventional manganese ferrite films processed by pulsed laser ablation (PLD), artificial ferrites that are constructed by a unique layer-by-layer PLD deposition were found to have inversion parameters as high as 58%. Magnetic properties of these ferrite films are compared as a function of cation inversion.

Index Terms—Artificial film, extended X-ray absorption fine structure (EXAFS), laser ablation deposition, spinel ferrite.

I. INTRODUCTION

MANGANESE ferrite (MnFe_2O_4) adopts the spinel structure, in which Mn and Fe ions are distributed between 8 of 64 tetrahedral sites (A sites) and 16 of 32 octahedral sites (B sites) in a unit cell. It is important to note that although there are the same number of divalent metal ions as A sites and as many trivalent metal ions as B sites, it does not need to follow that the divalent ions must reside on A sites and trivalent ions must reside on B sites. A typical manganese ferrite is on average 20% inverted when prepared using conventional ceramic processing techniques [1], which means an average of 20% of Mn ions reside on B sites. In this paper, we have examined conventional and artificial manganese ferrite samples processed by the pulsed laser ablation deposition (PLD) growth technique, in which the percentage of Mn ions on B sites can be artificially controlled.

Since the cation distribution on the available sites to a large extent decides the magnetic and electronic properties of the material, determining the site occupancy is a necessary first step in understanding newly developed ferrites. Here extended X-ray absorption fine structure (EXAFS) spectroscopy has been

used to quantitatively extract this information. The analysis of cation distribution by EXAFS was first performed by Harris *et al.* in 1996 [2]. This approach has been extended by Calvin who in 2002 performed the first multiedge refinement of the spinel structure [3]. Both Harris *et al.* and Calvin *et al.* made use of theoretical standards generated by the FEFF codes of Rehr *et al.* [4] together with the well established EXAFS refinement procedures outlined by Sayers and Bunker in [5].

II. EXPERIMENT

A. Pulsed Laser Growth of Conventional and Artificial Ferrites

In this experiment, there are a total of four samples grown by PLD which include conventional and artificial manganese ferrites grown on single crystal (111) and (100) MgO. The manganese ferrite which was deposited by the sequential ablation of two separate targets of MnO and Fe_2O_3 is referred to “artificial” ferrite films. In this process, each cycle consist of 4 laser pulses at 400 mJ incident upon the MnO target and 8 pulses on the Fe_2O_3 target. The substrate temperature was maintained at 700 °C. MnO and Fe_2O_3 layers were deposited alternately to produce films whose lattice constant and composition were nearly identical to those films grown using the conventional approach to PLD. The conventional approach entailed deposition from a single target of MnFe_2O_4 . Deposition on MgO (111) plane simulates the crystal structure of MnFe_2O_4 , where A and B sites are parallel to each other and the (111) plane. However, deposition on (100) MgO substrate would simulate a partial inverse spinel ferrite structure. The film thicknesses for this series range from 0.5 to 0.8 μm .

B. Extended X-Ray Absorption Fine Structure

X-ray absorption spectra were collected at the National Synchrotron Light Source using the beamline X23B. The design and optical performance of this beamline is presented in [6]. Data collection was performed in total electron yield at room temperature under standard conditions [7]. For each film sample, 3 to 5 sets of data were collected and merged during analysis. The raw experimental data in energy space was reduced to photoelectron wave vector space and then Fourier transformed to radial coordinates. These processing steps were performed using the Athena codes of Ravel [8]. Theoretical standards were generated by FEFF6 [4]. For each of the cations, standards were generated where the cation occupied octahedral and tetrahedral sites.

Manuscript received October 15, 2003. This work was supported in part by the U.S. National Science Foundation under award DMR-0226544. This work was performed in part at the National Synchrotron Light Source which is sponsored by the Department of Energy.

A. Yang is with the Department of Electrical and Computer Engineering, Northeastern University, Boston, MA 02115 USA (e-mail: fyang@ece.neu.edu).

V. G. Harris is with the Department of Electrical and Computer Engineering, Northeastern University, Boston, MA 02115 USA.

S. Calvin is with the Physics Department, Sarah Lawrence College, Bronxville, NY 10708 USA.

X. Zuo is with the Physics Department, Northeastern University, Boston, MA 02115 USA.

C. Vittoria is with the Department of Electrical and Computer Engineering, Northeastern University, Boston, MA 02115 USA.

Digital Object Identifier 10.1109/TMAG.2004.832246

All Fourier transforms were performed using Hanning windows having sills of 1 \AA^{-1} . The k -range for manganese edge and iron edge were the same at $4.0\text{--}12.0 \text{ \AA}^{-1}$. Each set of data was merged in energy space whereas the least-squares fit was performed in r -space over the range $1\text{--}6 \text{ \AA}$. A constrained model for the spinel structure was constructed by choosing several constraints that include:

- 1) Stoichiometry was constrained by the nominal fraction of metals, which was used to constrain the site occupancies of the cations, and the fractional difference in the metal-oxygen ion pairs in the first shell.
- 2) All multiple scattering paths were constrained according to the method described in [9]. Since any multiple-scattering path must be made up of some combination of direct-scattering paths, the parameters associated with multiple-scattering paths are dependent on those for direct-scattering paths.
- 3) Mean-square displacements (MSDs) and fractional changes in first shell metal-oxygen distances were assumed to be the same for both octahedral and tetrahedral sites occupied by the same ions. All outer shells were assumed to have the same MSDs, regardless of the cation species.

There are totally 11 independent variables, with 48 independent points altogether to build up the fit. The independent variables are: lattice parameter a , oxygen parameter u , fractional difference in the distance between iron-oxygen in the first shell, MSD for each metal with its first shell oxygens, MSD for all outer-shell paths, site occupancy of iron, amplitude reduction factor S_0^2 for each element, and inner potential shift ΔE_0 for each metal ion edge.

III. RESULTS AND DISCUSSION

A. Extended X-Ray Absorption Fine Structure

The real part of Fourier transform of EXAFS data and fits are presented in Figs. 1 and 2. The comparison between best fit and experimental data is excellent with R factors ranging from 0.02 to 0.03: values which are considered indicative of a constrained model that contains only small differences in detail with the experimental data. The EXAFS R-factor is a measure of the mismatch between data and best fit normalized by the amplitude of the data. Correlation between the EXAFS fitted variables are all below 0.85 suggesting that the adjustable parameters are not strongly coupled. EXAFS parameters determined by the best fit model are given in Table I. Since the samples are measured to be pure-phase spinel under XRD analysis, it is likely that the differences between the fit and experimental data arise from the various constraints used in our model. Amplitude reduction factors (S_0^2) represent the central atom shake-up and shake-off effects [5], is between 0.80 and 1.05 for both edges for all the samples. It is noted that the first shell MSD values are comparable to outer shells for iron. As for manganese, it is found to be smaller in conventionally grown samples but comparable in the artificial samples. This may be related to the site and valence disorder.

It is shown in the fitted parameters that manganese octahedral percentage is around 60 in the artificial manganese ferrite.

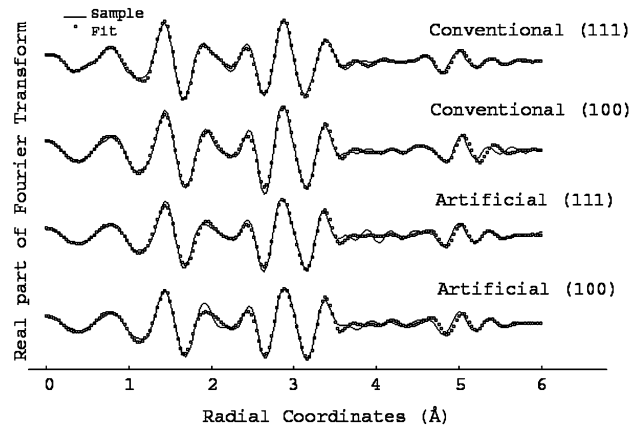


Fig. 1. Real part of Fourier transform of Fe EXAFS data and fits.

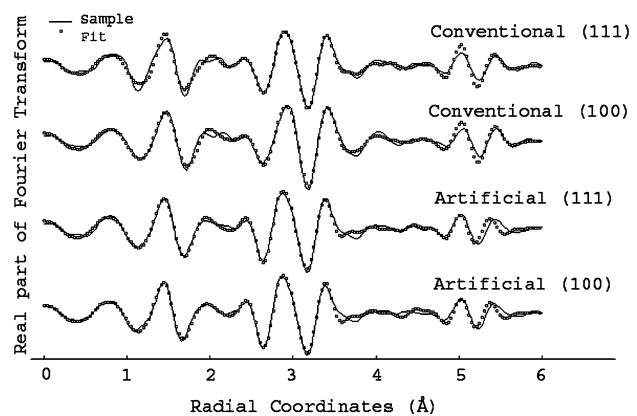


Fig. 2. Real part of Fourier transform of Mn EXAFS data and fits.

Even the conventionally grown manganese ferrite the inversion was 40–50% octahedral. The difference between the conventional ferrite and ceramic standards could result from its film structure or the nonequilibrium nature of the PLD preparation technique. There appears to be a trend in the first shell distortion in that the artificially grown films display a contraction of the near neighbor ions.

X-ray diffraction (XRD) was performed on both conventional and artificial films. From XRD data, the films clearly show strong crystal texture suggesting a pure phase spinel with lattice constants equal to 8.513 \AA and 8.533 \AA for (111) and (100) films, respectively. The conventional films showed the same XRD pattern as the artificial films with lattice constants equal to 8.506 \AA and 8.588 \AA for (111) and (100) films, respectively. This is compared to 8.511 \AA for the bulk Mn-ferrite [10]. Compared with the lattice parameters we got in EXAFS analysis as seen in Table I, the results are similar and differences fall within the expected range defined by the calculation uncertainty.

B. Magnetic Properties

Magnetic characterization of the manganese ferrite was performed using a vibrating sample magnetometer (VSM) and ferromagnetic resonance (FMR) spectrometer. VSM measurements were performed as a function of temperature and field strength, while FMR measurements were performed as a function of frequency and external field strength and

TABLE I
RESULTS OF FITTING EXAFS DATA TO A
THEORETICAL STANDARD UNCERTAINTIES IN THE LEAST SIGNIFICANT DIGIT
ARE GIVEN IN PARENTHESES

	Conventional (111)	Artificial (111)	Conventional (100)	Artificial (100)
Lattice Parameter (Å)	8.542 (2)	8.512 (2)	8.575 (2)	8.514 (1)
Oxygen Parameter	0.3951 (7)	0.3943 (4)	0.3939 (7)	0.3950 (4)
S_0^{-2}				
Manganese	0.82 (7)	0.83 (5)	1.02 (8)	0.91(8)
Iron	0.83(7)	0.73 (5)	0.97 (9)	0.82 (7)
Octahedral (%)				
Manganese (calculated)	53.55 (4)	57.28 (3)	47.77 (3)	57.75 (3)
Iron	73.13	71.29	75.97	71.06
First-shell distortion:				
Manganese (calculated)	0.0038	-0.0025	-0.0022	-0.0040
Iron	-0.002(4)	0.001 (2)	0.001 (4)	0.002(3)
Outer MSD (Å ²)	0.008 (1)	0.0076 (6)	0.009 (1)	0.0085 (8)
First-shell MSD (Å ²):				
Manganese	0.004 (2)	0.005(1)	0.005 (2)	0.005 (2)
Iron	0.005 (1)	0.005(1)	0.009(2)	0.006 (1)
R-factor	0.030145811	0.022396857	0.024393383	0.0302

TABLE II
PROPERTIES OF CONVENTIONAL AND ARTIFICIAL FILMS

	Conventional (111)	Artificial (111)	Conventional (100)	Artificial (100)
Lattice Parameter				
a (Å)	8.506	8.513	8.588	8.534
Saturation Magnetization $4\pi M_s^{RT}$ (kG)	3.0	2.6	2.5	2.0
Anisotropy Field H_A (kOe)	0.2	0.16	0.5	2.4
FMR linewidth ΔH (Oe)	200	40	260	400
Neel Temperature T_N (°K)	583	523	585	512
Exchange constants				
J_{AB} (°K)	-17.3	-15.6	----	-20.5
J_{BB} (°K)	15.2	13.5	----	0.7

orientation. The results of these measurements are presented in Table II.

In comparison to the PLD single crystal films (conventionally grown), the artificial ferrites grown on (111) are measured to have a smaller anisotropy field (160 Oe vs. 200–500 Oe) and a remarkably reduced FMR linewidth (40 Oe compared with 200–260 Oe). When the artificial ferrite is grown on (100) MgO, an increase in ΔH to 400 Oe and the anisotropy field to 2400 Oe were measured. We speculate that the effects measured in the (100) MgO films are due to a tetragonal distortion of the unit cell that is supported by both XRD and EXAFS in the measurement of a reduced lattice parameter and a contraction of the near neighbor ions between the artificial and conventionally grown samples. This may be the result of a Jahn-Teller distortion caused by the increase in Mn^{+3} on the B-sublattice.

Compared with the theoretical $4\pi M_s$ of manganese ferrite bulk, i.e., 4 kG at room temperature [1], both artificial and conventional films have reduced $4\pi M_s$ values. In addition, the Neel temperatures for the artificial films are substantially lower than those of the conventional films with the latter identical to that reported for a single crystal of $MnFe_2O_4$ [11]. Both of these trends are consistent with the larger Mn cation inversion measured by EXAFS in both the conventional and artificial films. Finally, the calculated values of J_{AB} and J_{BB} for the conventional films are comparable to values determined by Mössbauer Effect spectroscopy ($J_{AB} = -20.7$ K and $J_{BB} = 13.7$ K) [12]. For the artificial (100) film we calculate a reduced value 0.7 K for J_{BB} consistent with a reduced $4\pi M_s$. We attribute the changes in T_N and $4\pi M_s$ to an increase in Mn^{+3} on the B sublattice. It is as yet unclear the impact of local distortions on the magnetization of these materials where slight changes in bond angles can have an adversely large impact on the magnetic properties.

REFERENCES

- [1] J. Smit and H. P. J. Wijn, *Ferrites*. New York, NY: Wiley, 1959, ch. VIII, p. 144.
- [2] V. G. Harris, N. C. Koon, C. M. Williams, Q. Zhang, M. Abe, and J. P. Kirkland, "Cation distribution in NiZn-ferrite films via extended x-ray absorption fine structure," *Appl. Phys. Lett.*, vol. 68, pp. 2082–00, 1996.
- [3] S. Calvin, E. E. Carpenter, V. G. Harris, and S. Morrison, "Use of multiple-edge refinement of extended x-ray absorption fine structure to determine site occupancy in mixed ferrite nanoparticles," *Appl. Phys. Lett.*, vol. 81, p. 3828, 2002.
- [4] J. J. Rehr, S. I. Zabinsky, and R. C. Albers, "High-order multiple-scattering calculations of x-ray-absorption fine structure," *Phys. Rev. Lett.*, vol. 81, p. 3828, 2002.
- [5] D. E. Sayers and B. A. Bunker, *X-ray Absorption: Principles, Applications, Techniques of EXAFS, SEXAFS, and XANES*. New York, NY: Wiley, 1988, vol. 92, pp. 211–253.
- [6] R. A. Neiser, J. P. Kirkland, W. T. Elam, and S. Sampath, "Optical performance of the Naval Research Laboratory's materials analysis beamline at the NSLS," *Nucl. Instrum. Meth. Phys. Res.*, vol. A266, p. 220, 1988.
- [7] *Data Collection was Performed Using a Total Electron Yield Technique at Beamline X23B at the National Synchrotron Light Source*. At the time data were collected the storage ring energy was 2.54 GeV and the ring current ranged from 180–250 mA.
- [8] B. Ravel, *Proc. 12th Annu. XAFS Conf.*
- [9] S. Calvin, "Relationship Between Electron Delocalization and Asymmetry of the Pair Distribution Function as Determined by x-ray Absorption Spectroscopy," Ph.D. dissertation, City University of New York, 2001.
- [10] R. W. G. Wyckoff, *Crystal Structures*, 2nd ed. New York, NY: Interscience, 1965, vol. 3, p. 79.
- [11] R. Vautier and M. Paulus, "Mn-Fe³⁺ spinels (Mn ferrites) and Mn-Fe³⁺ spinels with substitutions," in *Landolt-Börnstein Numerical Data and Functional Relationship*, K.-H. Hellwege and A. M. Hellwege, Eds. Berlin, Germany: Springer-Verlag, 1970, vol. 4, p. 158.
- [12] G. A. Sawatzky, F. Van Der Woude, and A. H. Morrish, "Mössbauer study of several ferromagnetic spinels," *Phys. Rev.*, vol. 187, no. 2, p. 747, 1969.